Sonochemical Design of Engineered Gold–Silver Nanoparticles

ARTICLE *in* THE JOURNAL OF PHYSICAL CHEMISTRY C · JANUARY 2008

Impact Factor: 4.77 · DOI: 10.1021/jp710535r

Sonochemical Design of Engineered Gold−Silver Nanoparticles

Darya Radziuk, Dmitry Shchukin,* and Helmuth Möhwald

Max-Planck Institute of Colloids and Interfaces, D14424 Potsdam, Germany

Received: November 1, 2007; In Final Form: December 7, 2007

The sonochemical technique includes the application of ultrasound (20 kHz, 500 W) to a medium as a pressure wave resulting in cavitation in it. The implosive collapse of vapor microbubbles (cavities) creates shock waves with extremely high physical forces for modification of gold nanoparticles. Stable monodisperse gold nanoparticles with a diameter of 30 nm produced by the titration method were used as initial templates. These formed gold nanoparticles mixed with the surfactants (sodium borohydride in water; poly(vinyl pyrrolidone) in ethylene glycol; poly(ethylene glycol); sodium dodecyl sulfate in water or propanol) were added into the pre-sonicated silver solution and then were sonicated again. Transmission electron microscopy, electron and wide-angle X-ray diffraction accompanied with UV−vis absorption spectroscopy data revealed that only 10 min of ultrasonic irradiation was enough to form monodisperse polygonal gold−silver structures. More than 1 h of ultrasonic treatment was required to create gold−silver worms or netlike nanostructures capped with sodium dodecyl sulfate. Gold−silver nanocomposites produced in presence of any surfactant dramatically increased their size. The most, pronounced effect of this increase was noticed for worm- or netlike gold−silver nanocomposites fabricated in the presence of sodium dodecyl sulfate either in propanol or in water.

Introduction

Gold nanoparticles received much attention since Michael Faraday reported a systematic study of the synthesis of colloidal gold in 1857.[1] Monodisperse, spherical gold nanoparticles are produced in a liquid by reduction of hydrogen tetrachloroaurate ($HAuCl_4$) with sodium citrate. Pioneered monodisperse gold nanoparticles were prepared employing the "citrate" method by J. Turkevitch et al.[2] in 1951 and G. Frens in 1973.[3] Due to the unique size-dependent optical properties, gold particles are widely employed in microelectronic, optoelectronic, or magnetic devices.[4] Malleable gold is known to be affected neither by air nor most reagents.

To increase the electrical and thermal conductivity and optical reflectivity, gold is usually coupled with silver. Silver nanoparticles are usually produced in the presence of silver salt (silver nitrate) via reduction by sodium borohydride which can be used for both gold and silver particles for their reduction and stabilization.[5] The absorption bandwidth of gold or silver has a relatively broad bandwidth in the visible wavelength range. The crystal structure of both metals is very similar to each other. Moreover, the fact that gold is insoluble in nitric acid and preserves its chemical properties under heat, moisture, oxygen, and most corrosive reagents lends gold−silver composites perspectives for ergonomic electronic contacts, ultrafast data communication, and optical data storage. The size and shape of gold−silver nanoparticles are strongly dependent on the method and experimental conditions. In spite of the relatively high stability of the created gold−silver nanocomposites prepared using such traditional methods as the reduction by sodium borohydride of supported metal salts,[6] citrate[7] or hydrazine reduction,[8] these methods do not result in shape control of bimetallic nanoparticles with tuneable structure. This is mainly because of the poor energy supply delivered from reactants to reduce both gold and silver ions and to design their surfaces during chemical reactions overcoming the interfacial energies and interactions.

Attempts to form gold−silver nanorods in bulk solution at ambient conditions failed due to the higher concentrations of metal salt required during the growth phase, in which the precipitation of silver chloride cannot be avoided.[9] The only published way to make composite structures is to prepare core−shell structures in a two-step synthesis. According to Chen and Nickel[10] both silver−gold and gold−silver with core−shell structure were produced in a two-step chemical reaction in the mixture of silver colloids and tetrahydrochloroaurate. Gold and silver are miscible in all proportions, due to the almost identical lattice constants, but differ in both redox potentials and surface energies. For this reason silver seeds are easily prepared via reduction in silver nitrate by $NaBH_4$ and gold ones via reduction in $HAuCl_4$ in poly(vinyl pyrrolidone) or in alcohol, or their derivatives with longer chains.

Recently, either hollow or filled bimetallic nanocomposites have been sonochemically prepared. The sonochemical technique includes the application of ultrasound for the delivery of energy into the reaction mixture. The sound of high frequency (from 20 kHz to several MHz) is transmitted through a medium as a pressure wave and induces a vibrational motion of the molecules through it. The series of compression waves attenuated by stretching waves create cavities inside the bulk solution. Millions of microscopic bubbles expand during the negative pressure excursion and implode violently during the positive one. The cavitational collapse lasts a few microseconds, and the amount of energy released by each individual bubble in a minute is extremely high. Unlike the traditional energy sources such as heat, light, or ionizing radiation, ultrasonic irradiation creates local temperatures from 1900 to 5200 K, pressures of

* To whom correspondence should be addressed. E-mail: Dmitry.Shchukin@mpikg.mpg.de. Telephone: +49 (0)331-567-9781. Fax: +49 (0)331-567-9202.

10.1021/jp710535r CCC: $40.75
Published on Web 01/29/2008

about 10^3 atm with heating/cooling rates above 10^8 K·s^{-1}.[11] Thus, the extremely high physical parameters make ultrasound a powerful tool for thermal chemical reactions inside the bulk solution at room temperature. The power of ultrasound is used for a variety of purposes including welding,[12] rupturing cell walls,[13] and dispersing solids in liquids.[14]

Stable colloidal silver was first produced in aqueous silver nitrate under ultrasonic treatment (20 kHz) by Nagata[15] in 1992. Colloidal gold particles in aqueous $HAuCl_4$ were reported later in 1993 by Grieser.[16] Further experiments applying ultrasound have been mostly employed for preparation of iron colloids,[17] hollow nanospheres and nanocrystals,[18] semiconductor nanoparticles,[19] core−shell microspheres,[20] gold nanoparticles in water,[21] colloidal Pt,[22] amorphous silver,[23] or decomposition of volatile organometallic materials in the presence of stabilizers.[24]

For sonochemically formed (20 kHz) metal nanoparticles with sizes of only several nanometers, ultrasonic cavitation leads to a significant change in morphology without affecting chemical reactions.[25] Recently stable gold nanoprisms with triangular or hexagonal shape (30−40 nm in planar dimension and 6−10 nm in thickness) were grown via ultrasound in ethylene glycol (EG) solution.[26,27] Fuchigami synthesized spherical gold nanoparticles by applying ultrasonication to the aqueous solution with $HAuCl_4$ in sodium dodecyl sulfate (SDS).[28] The sonochemical reduction of gold nanoparticles at the frequencies of 20, 213, 647, or 1062 kHz in $HAuCl_4$ solution with small amounts of 1-propanol was performed by Okitsu in 2005.[21] Generally, poly(vinyl pyrrolidone) (PVP) is commonly employed in these experiments as a good reductant of gold ions, inhibiting the aggregation of the resulting nanoparticles. However, to the best of our knowledge there is no data about the surface modification of gold−silver composites under ultrasonic treatment.

In this paper we examine the influence of the ultrasonic treatment at a constant frequency of 20 kHz with varying the output power up to 500 W on the shape and state of formed gold nanoparticles (Au NPs) in silver salt solution. Silver nitrate was mixed with one of the following reductants: sodium borohydride water solution, or poly(vinyl pyrrolidone) in ethylene glycol, or poly(ethylene glycol) (PEG) water solution, or sodium dodecyl sulfate dissolved in water and propanol. The mixtures were sonicated first at output power of ultrasound at 250 W for at least 30 min and then at 450 W for less than 1 h either under argon atmosphere or not. UV−vis spectroscopy, transmission electron microscopy, electron and wide-angle X-ray diffraction (WAXD) were involved to characterize the structure of ultrasonically created novel gold−silver nanocomposites.

Experimental Section

Materials. Hydrogen tetrachloroaurate (III) trihydrate ($HAuCl_4$·$3H_2O$, 99.99%) and sodium *n*-dodecyl sulfate (SDS, 99%) were purchased from Alfa Aesar (Germany). Silver nitrate ($AgNO_3$, 99.8%), sodium borohydride ($NaBH_4$, 98%), sodium citrate ($Na_3C_6H_5O_7$), poly(ethylene glycol) (PEG, 8 kDa), ethylene glycol (EG, 99%), and poly(vinyl pyrrolidone) K-30 (PVP K-30, 40 kDa) were obtained from Aldrich (Germany). Propanol (>99%) was bought from Merck (Germany). The water used in all experiments was prepared in a three-stage Millipore Milli-Q Plus 185 purification system, and had a resistivity higher than 18.2 MΩ·cm^{-1}.

Synthesis of Gold Nanoparticles. Gold nanoparticles were produced according to the "citration" method originally proposed by Turkevitch[2] and then repeated by Frens and Sutherland.[3] The procedure was carried out in a 1 L round-bottom flask, prewashed in concentrated hydrochloric acid, rinsed in triply distilled water, and oven-dried prior to use. For the synthesis of gold nanoparticles 500 mL of 1 mmol/L $HAuCl_4$ was brought to a rolling boiling with vigorous stirring. Fresh 50 mL of 38.8 mmol/L sodium citrate was rapidly added, and the solution resulted in a color change from pale-yellow to burgundy. Boiling was continued for 10 min, then the heating mantle was removed, and stirring lasted for additional 15 min. After the solution reached room temperature, it was dialyzed for 24 h through a cellulose dialyzing tube Conatex Didactic against deionized water. To avoid the influence of light, the final gold solution was kept in darkness at room temperature. No sediment was observed during a month.

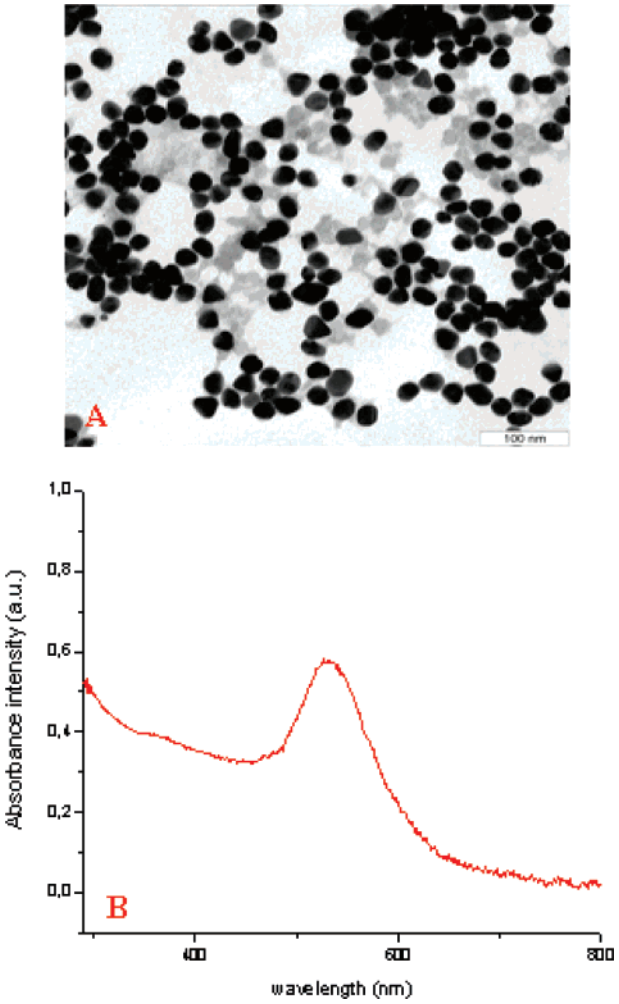

Figure 1. (a) TEM image and (b) UV−vis absorption spectra of gold nanoparticles formed via the citration method based on the procedure of Turkevitch et al.[2]

Ultrasonic Treatment of Gold−Silver Nanocomposites. Sonication was performed by the Ultrasonic Processor VCX 505 (CV 33) Sonics & Materials (Newtown, U.S.A.) Inc. operating at 20 kHz with maximal output power of 500 W. The sonication of formed gold nanoparticles was carried out in the presence of:

(a) Sodium Borohydride in Water Solution. The resulting solution was sonicated at constant frequency of 20 kHz in two steps first at 250 W and then at 450 W. A 30 mL volume of 40 mmol/L concentration of $AgNO_3$ was sonicated at 250 W for 15 min. Then, 30 mL of a 5 mmol/L concentration of gold nanoparticles was added into the previous solution, and the mixture was sonicated at 450 W for 45 min. When the ultrasonic treatment was finished, the sonicated solution was mixed with 5 mL of 7 mmol/L concentration of $NaBH_4$. The color of the

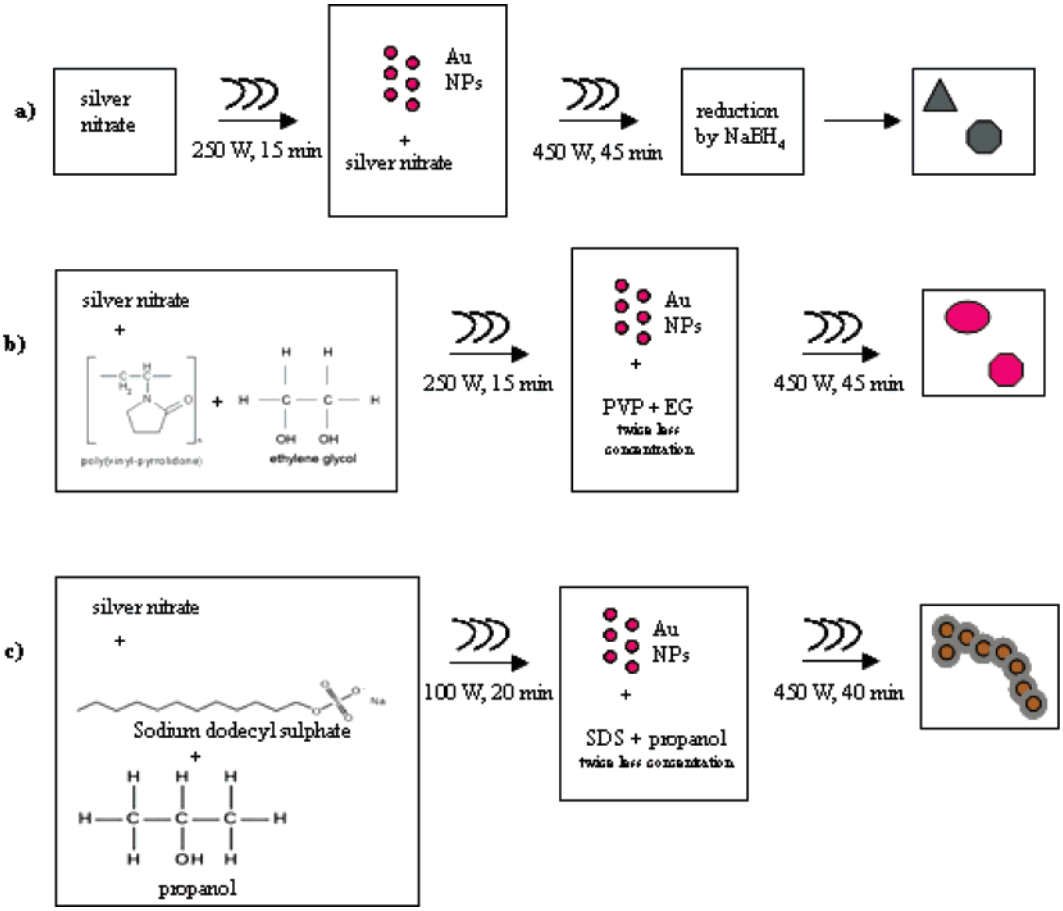

Figure 2. Scheme of sonication employed for the preparation of (a) triangular or polygonal gold−silver nanostructures with the reduction by $NaBH_4$; (b) spherical or multiangular gold−silver nanocomposites in the presence of poly(vinyl pyrrolidone) in ethylene glycol; and (c) worm-like gold−silver nanocomplexes capped with sodium dodecyl sulfate in propanol.

final solution was violet. The dark sediment appeared on the bottom of the flask on the next day after ultrasonic treatment at room temperature.

(b) Poly(vinyl pirrolidone) in Ethylene Glycol Solution. In 30 mL of ethylene glycol 200 mg of poly(vinyl pirrolidone) was stirred overnight. To this organic mixture was added 15 mL of 40 mmol/L $AgNO_3$, and the mixture was ultrasonically irradiated during 15 min at 250 W. After the first step of ultrasonic treatment, 15 mL of a 5 mmol/L concentration of Au NPs previously dissolved in 100 mg of PVP was added to the sonicated solution. The final mixture was treated at 450 W for 45 min. A strong rapid heating of the glass flask and intensive evaporation of the solution were observed during the sonication of the solution. The resulting solution turned from a light-brown to a light-gray color. On the next day after ultrasonic treatment dark sediment appeared on the bottom of the flask.

(c) Poly(ethylene glycol) in Water Solution. The mixture of 30 mL of 2 mg/mL aqueous PEG and 7.5 mL of 40 mmol/L $AgNO_3$ was sonicated at 250 W for 30 min. Then 7.5 mL of Au NPs was added into the solution, and ultrasonic treatment continued at 450 W for 45 min. The ultrasonic treatment was carried out in argon at each step of sonication. The resulting solution appeared transparent with strong white foam on the top and dark-gray precipitation on the bottom.

(d) Sodium Dodecyl Sulfate in Water Solution. For 10 min, 200 mg of SDS in 86.5 mL of H_2O was stirred; 30 mL of this solution was added to 7.5 mL of 40 mmol/L $AgNO_3$ and sonicated at 250 W for 30 min; 7.5 mL of Au NPs was mixed with 100 mg of SDS, shaken for 15 min, and then added to the solution for treatment at 450 W for 30 min. Strong foam appeared during the ultrasonication. The final solution became roily, and its color changed into light violet.

(e) Sodium Dodecyl Sulfate in Propanol Solution. In 30 mL of propanol was dissolved 200 mg of SDS and stirred 10 min in conical glass. Then the mixture was added to 6 mL of 40 mmol/L $AgNO_3$ and sonicated at 100 W for 20 min. The ultrasonic treatment created strong white foam, and the solution became milky. As soon as the sonication was completed, 1.5 mL of 5 mmol/L Au NPs and 100 mg of SDS were added, and then the mixture was sonicated at 450 W for 40 min. Each step of ultrasonic treatment was carried out in argon. The final solution had a light-magenta color. No precipitation was observed.

Characterization. The electrophoretic mobility of freshly produced gold nanoparticles was measured employing a Zeta Sizer (Malvern Instruments). The intensity of the absorption peaks and spectral bandwidth of the original gold nanoparticles and their composites were examined by a Varian CARY 50 Conc UV−vis spectrophotometer. The size and the polydispersity of both the gold nanoparticles and gold−silver nanocomposites were estimated employing Zeiss EM 912 Omega transmission electron microscope (TEM) and a high performance particle sizer (Malvern Instruments) for dynamic light scattering. The phase crystal structure and content of the gold−silver composites were examined by a D8 Bruker wide-angle X-ray diffractometer (WAXD).

Results and Discussion

Gold nanoparticles were prepared via the titration method based on the paper of Turkevitch.[2] The final Au NPs have a

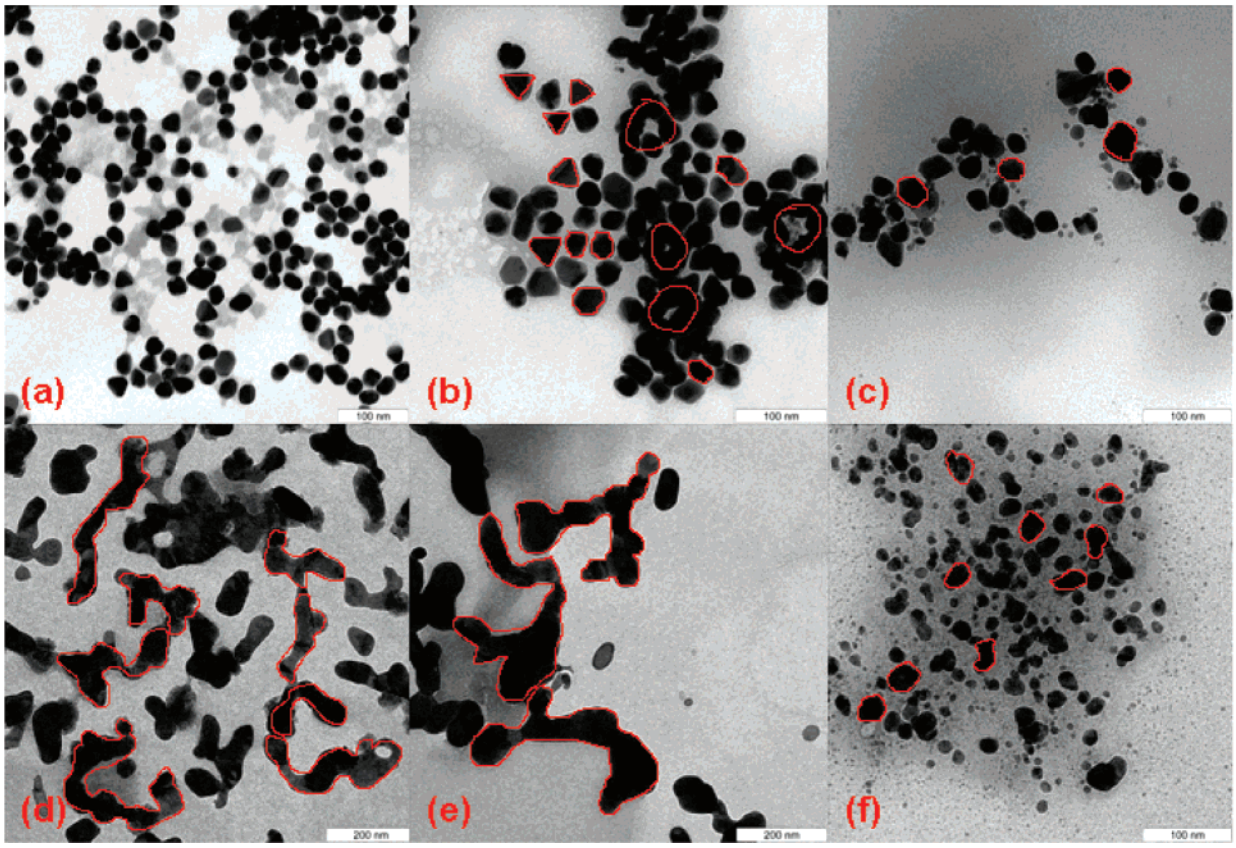

Figure 3. Transmission electron microscopy images of (a) the control gold nanoparticles; (b) gold−silver nanostructures formed after sonication of the gold nanoparticles in the water solution of silver nitrate (at 450 W for 45 min) and reduction with sodium borohydride; (c) gold−silver composites after sonication of gold nanoparticles in the presence of silver nitrate and poly(vinyl pyrrolidone) in ethylene glycol (at 250 W for 15 min and 450 W for 45 min); (d) gold−silver composites after sonication of gold nanoparticles in the presence of silver nitrate and sodium dodecyl sulfate in propanol (at 100 W for 20 min and 450 W for 40 min); and (e) water (at 250 W for 30 min and 450 W for 30 min); (f) gold−silver composites after sonication of gold nanoparticles in the presence of silver nitrate and poly(ethylene glycol) (at 250 W for 30 min and 450 W for 45 min).

diameter of (30 ± 3 nm) with negative ξ potential of −57.1 ± 8.9 mV. No visible sediment and no change in color of gold NPs appeared for at least a month of storing at room temperature. Transmission electron microscopy images revealed monodisperse spherical nanoparticles (Figure 1a). The UV−vis absorption spectrum (Figure 1b) indicates a relatively narrow absorption peak near 560 nm, corresponding to the characteristic wavelength of gold NPs. The 30 nm diameter of the resulting gold nanoparticles appeared optimal for the examination of the influence of the ultrasonic treatment for the modification of Au NPs with silver in the presence of various reductants and surface-active agents.

The mechanism of the interaction between the high-frequency acoustic wave and the heterogeneous water solution is as following. At the very beginning the sinusoidal ultrasonic waves shock the liquid, which results in cycles of water compression and expansion. On their way of longitudinal propagation the acoustic waves excite the points with prior dissolved gas (cavitation nuclei), thus giving birth to either the vapor or gas-filled bubbles inside the bulk solution. Since the gas inside extends, the bubbles grow under negative pressure. Then during the compression cycle the bubbles become smaller due to the positive pressure. Since the volume of gas decreases, the internal energy of the bubbles increases, thus making the bubbles grow again during the following expansion phase. The growth of cavities strongly depends on the surface tension of the liquid/gas interface and gas macro parameters such as pressure and temperature which depend on time. As soon as the radius of the bubbles reaches its maximum value, the bubbles implode. Microjet impact and shock-wave damage appear as a result of this collapse. The deformation of the cavitation bubbles increases due to the asymmetry of the surrounding medium near the interface which results in a liquid stream through the surface of the cavities (microjet impact). Turbulent jet impact and shock waves have a sufficient energy to produce the head-on collision of gold and silver ions accompanied by surfactants to produce gold−silver alloys in the bulk solution at room temperature.

Actually, two procedures of ultrasonic treatment are involved to influence the chemical reactions—simultaneous and successive methods. The successive one is more effective for formation of the gold−silver nanoalloys. The duration of the ultrasonication is shorter in the first part of sonication and longer in the second one. During the first step of ultrasonic treatment the reduction of silver ions without Au NPs occurred. As the sonication accelerates the thermodynamic processes in the bulk solution, the absence of gold nanoparticles prevents their undesirable aggregation during irradiation. Before the second part of ultrasonic treatment the Au NPs were mixed up with surfactants and then added to the previously sonicated solution with partly reduced silver. The longer, later sonication provides the further reduction of silver in close contact with surface-stabilized Au NPs.

Here, the ultrasonic treatment performed by a continuous acoustic wave was carried out in two steps of sonication (Figure 2). The first one consists of ultrasonic treatment of either pure silver nitrate (Figure 2a) or silver nitrate mixed with poly(vinyl pyrrolidone) in ethylene glycol (Figure 2b), poly(ethylene glycol), sodium dodecyl sulfate in propanol (Figure 2c), or in

water at lower output power and shorter time of sonication (not more than 20 min). The second step includes the addition to the sonicated silver solution of the prepared gold nanoparticles either without (Figure 2a) or mixed with poly(vinyl pyrrolidone) in ethylene glycol (Figure 2b), poly(ethylene glycol), sodium dodecyl sulfate in propanol (Figure 2c), or in water of twice less concentration and their sonication at higher output power and longer time (at least 40 min). During the ultrasonic treatment in both steps the treated mixture was kept in ice to avoid the undesirable heating of the solution.

After sonication, the resulting solution of gold−silver nanocomposites in aqueous PEG and SDS water solution turned out transparent with dark gray sediment. The sediment with the same color appeared on the bottom of the glass vessel after addition of $NaBH_4$ to the sonicated gold−silver solution as soon as the ultrasonic treatment was completed. Although the final gold−silver nanocomposites in PVP with EG solution became transparent, the sediment was a pale magenta color. Gold−silver nanocomposites ultrasonically produced in SDS in propanol formed a small amount of dark sediment in the light-cognac solution after the sonication finished. There is a connection between the color of the solution and the size or shape of the formed particles. The appearance of the dark gray sediment indicates the access of silver rather than gold. In this way PEG and SDS in water as well as $NaBH_4$ influence stronger the silver ions, whereas PVP in ethylene glycol solution better stabilizes gold and reduces silver to a smaller degree. The intriguing cognac color can indicate the presence of both gold and silver at equal extents of reduction and stabilization.

The cavitation created acoustically influences indirectly the formation of gold−silver alloys. Although the rapid cooling/heating rates of bubbles provide the opportunity to release the extreme high energy after the implosion of the microbubbles, this energy diffuses rather like shock waves than microjet impact. For solid particles with the size in the nanometer range, jet formation cannot occur at the sound frequency of 20 kHz, because the resonant bubble size is much smaller than the distance corresponding to a microjet deformation. In this way the shock waves produced can drive gold particles and silver ions together at ultrafast velocities to melt them at the point of collision.

The degradation of the surfactants during the ultrasonic treatment allowed modification of the shape of gold nanoparticles in their interaction with silver ions. The TEM images revealed monodisperse gold nanoparticles that were more spherical and less triangular (Figure 3a). Au NPs sonicated in silver salt and afterward reduced by sodium borohydride increased their size and changed the shape rather to triangular or polygonal structure (Figure 3b). Moreover, the vapor rings of relatively small diameter and gold−silver particles in their interface were revealed. Multiangular nanocomposites of larger size appeared after ultrasonic irradiation of the gold−silver mixture in the presence of poly(vinyl pyrrolidone) in ethylene glycol (Figure 3c). Some of the particles are connected like beads, and the others exhibit a more than double increase in size. This is mainly due to the capping effect and the relatively low rate of degradation of PVP. The presence of ethylene glycol can enhance the interaction of the silver ions with gold nanoparticles and with PVP. The TEM analysis revealed wormlike complexes after sonication of the Au NPs in silver nitrate reduced by sodium dodecyl sulfate in propanol (Figure 3d). The particles aggregate in a wormlike shape which is stabilized by SDS (Figure 3e). In comparison with the previous gold−silver structures, in this case the great increase both in

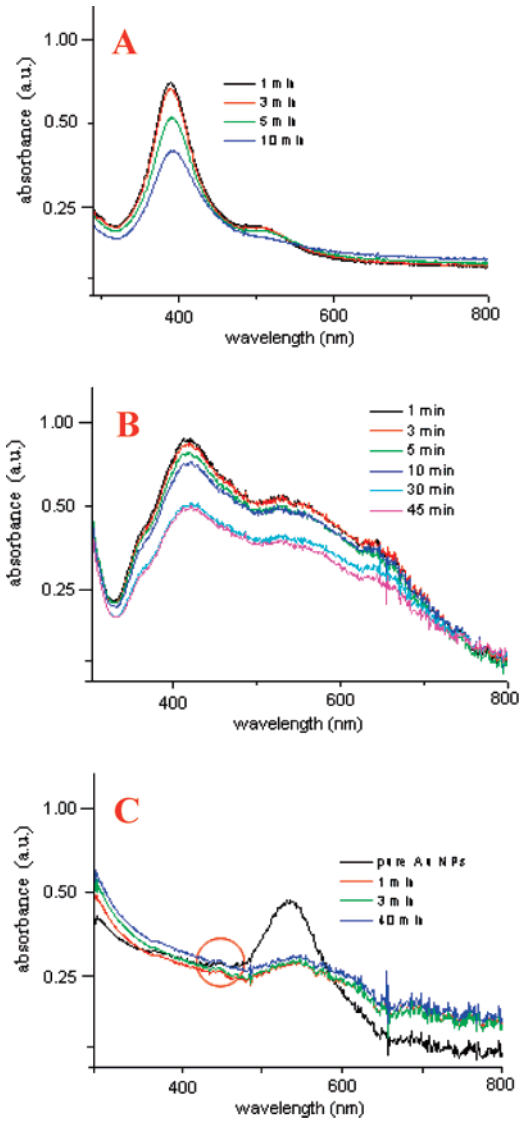

Figure 4. UV−vis absorption spectra of (a) gold−silver composites after sonication and reduction with $NaBH_4$, (b) in poly(vinyl pyrrolidone) in ethylene glycol and (c) sodium dodecyl sulfate in propanol.

size and width with the length increase of the formed metal worms is noticed. In addition, thick metal worms are more connected to each other, providing the net production of SDS capped and reduced metal nanocomposites rather in H_2O than in propanol. Uniformly distributed gold−silver round structures resulted after sonication in PEG (Figure 3f). PEG is known for acting as a good capping agent and stabilizer. In such a way the roundness and dispersity of formed bimetal nanocomposites are due to impairment of this polymer during the ultrasonic treatment.

According to the above-mentioned descriptions, the reduction with $NaBH_4$ of the silver on the gold surface after sonication results in monodisperse gold−silver alloys of triangular or polygonal structure. Ultrasonic treatment of alcoholic solutions can accelerate the interparticle collisions in the presence of such stabilizers as PVP and SDS. Because of the backbone complexion of SDS, Au−Ag nanoworms with varied lengths and widths can be formed during the ultrasonic treatment. Moreover, due to the perfect stabilizing effect of PEG, nice spherical gold−silver nanocomposites can result after sonication.

Application of the same procedure of ultrasonic treatment in the presence of various surfactants took different lengths of time for formation of the gold−silver nanoalloys. The UV−vis

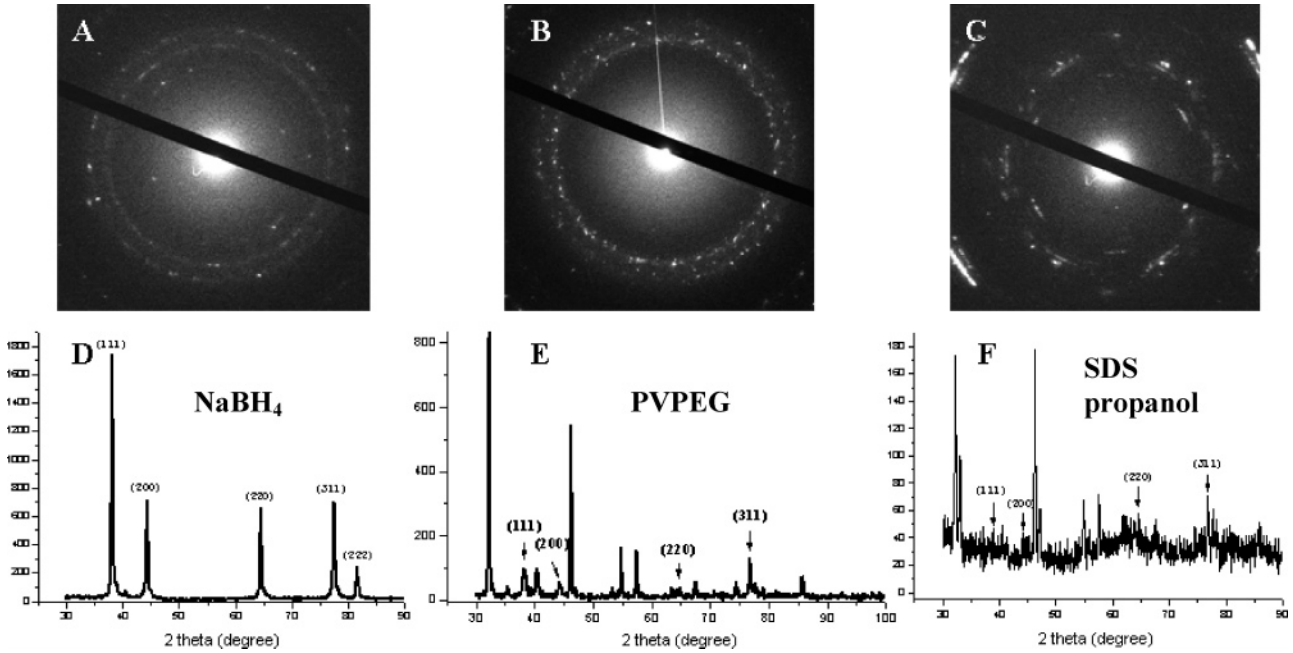

Figure 5. Electron diffraction diagrams (ED) and wide-angle X-ray diffraction patterns (WAXD) of the gold−silver alloys ultrasonically prepared with aqueous sodium borohydride (a, d), poly(vinyl pyrrolidone) in ethylene glycol (b, e), sodium dodecyl sulfate in propanol (c, f).

absorption analysis of the gold−silver solutions in the presence of aqueous $NaBH_4$, PVP in ethylene glycol, and SDS in propanol is monitored as shown in Figure 4. Parts a and b of Figure 4 revealed two resolved absorption peaks. The one near 400 nm corresponds to that of silver absorbance, while the peak near 560 nm coincides with the characteristic wavelength of gold absorbance. In both cases the silver absorption peak appeared with relatively larger intensity than that of the gold one. The absorption bandwidth increased with the duration of ultrasonic irradiation. At the same time the intensity of the absorption peaks for gold and silver also decreased. These changes reflect the speed of the formation of bimetallic complexes. Thus, one required maximally 10 min of ultrasonic treatment for the formation of gold−silver alloys with aqueous $NaBH_4$ and at least 45 min for this in the presence of PVP in EG.

However, the inverse spectroscopic result was noticed in the case of gold−silver alloys formed in the presence of SDS in propanol (Figure 4c). After several minutes of ultrasonic irradiation of the silver solution with Au, NPs inside only one broad absorption peak near 560 nm were detected. The longer sonication provided the appearance of one more badly resolved absorption peak which was detected near 430 nm. These point to the slow reduction of silver ions on the surface of gold nanoparticles capped with SDS.

In this way, one required less than 1 h of ultrasonic irradiation to reduce and stabilize gold−silver composites of round or multiangular structures in the presence of either PVP or PEG. However, only 10 min of sonication is enough for the reciprocal sticking of gold nanoparticles with partly reduced silver ions, resulting in monodisperse polygonal bimetallic nanoparticles after addition of aqueous sodium borohydride. A much longer time (more than 1 h) of ultrasonic irradiation is required to create gold−silver wormlike or netlike gold−silver nanostructures capped in between with SDS.

TEM and ED analysis (Figure 5a−c) were performed on separate nanoparticles. On the black background one can see white concentric rings that indicate the face-centered cubic (fcc) crystal structure of the samples and prove the presence of both gold and silver. In any ED pattern the rings are not solid and consist of either small, broken parts or white, nonuniform dashlike dots. Such lines of the rings specify the polycrystal objects with a limited number of crystal orientations. The intensity of the dots that form the rings in the case of $NaBH_4$ is greater than that in EG PVP and SDS with propanol that coincides with XRD analysis. This is due to the more frequent repetition of the reflectivity of the phase planes of the gold−silver crystals and, as a result of it, a more organized structure. In the case of $NaBH_4$ the lines of the rings are badly defined and resolved because of the relatively small size of the final gold−silver crystals in comparison with the other two. In Figure 5c the radius of the rings and the distance between the rings differ to a greater extent than in Figure 5a, b. Moreover, dash−dots are longer and thicker in the case of SDS with propanol. This fact proves the wormlike shape of final bimetallic particles. Monitoring the distance between the rings in this case can point to the distance between alloys capped with SDS. The distances between ED rings in the cases of $NaBH_4$ and EG PVP are almost the same and shorter than in the case of SDS in propanol. Comparing this with TEM analysis (Figure 3) one can conclude on the closer and smaller packing structure of gold−silver alloys formed by $NaBH_4$ or PVP in EG.

The X-ray diffraction patterns (XRD) exhibit diffraction peaks in the region of 2θ from 38° to 82° for the gold NPs with silver reduced in the presence of $NaBH_4$ (Figure 5d), PVP in ethylene glycol (Figure 5e), and SDS in propanol (Figure 5f). In the case of the reduction by $NaBH_4$ the XRD analysis indicated the most intense peaks (111) at $2\theta = 38°$, (200) at $2\theta = 44°$, (220) at $2\theta = 64°$, (311) at $2\theta = 77°$; the peaks with less intensity (222) at $2\theta = 81°$ coincide with those for both Au and Ag (Figure 5d). After ultrasonic irradiation of the gold NPs with silver atoms in the presence of PVP in EG the peaks (111) at $2\theta = 38°$ and (311) at $2\theta = 77°$ with higher intensity and (200) at $2\theta = 44°$ together with (220) at $2\theta = 64°$ with less intensity of diffraction have been detected (Figure 5e). The diffraction peaks are in good agreement with those for gold and silver. The most intense peaks (311) at $2\theta = 77°$ and (220) at $2\theta = 64°$ have been revealed for gold and silver with SDS in propanol (Figure 5f).

TABLE 1: XRD Data of Gold and Silver Nanocrystals

2-θ		intensity		D-spacing, Å	(*hkl*)
Au	Ag	Au	Ag	Au, Ag	Au, Ag
38.22	38.15	100.00	100.00	2.36	111
44.43	44.34	47.94	46.77	2.04	200
64.64	64.50	28.39	25.61	1.45	220
77.65	77.47	31.32	27.18	1.23	311
81.81	81.62	8.95	7.69	1.18	222

Detailed information on the obtained gold−silver crystal lattices can be found in Table 1.

Conclusion

Stable monodisperse gold nanoparticles with the average diameter of 30 nm were used for modification with ultrasound at room temperature. Due to the cavitation the rapid cooling/heating rates of bubbles give the opportunity to release extremely high energy after the implosive collapse of the microbubbles produced at 20 kHz; this energy is diffused rather like shock waves than microjet impact. The reason for this is the strong surface dependence of microjet deformations formed by the implosion of the bubbles in comparison with the resonant bubble size. Following this, the main driving force in the solution is the appearance of shock waves that impose ultrafast velocities to gold particles and silver ions to merge them at the point of collision. The prepared gold nanoparticles were mixed with silver salt and sonicated step-by-step successively. The successive ultrasonic treatment was found as the optimal one because it helps to avoid undesirable aggregation of gold nanoparticles and partly reduces silver ions during the sonication. The type of surfactant influences the size and shape of gold−silver alloys as well as the duration of the ultrasonic treatment for the complete reduction of silver ions on the gold surface. Only 10 min of sonication is enough to form monodisperse polygonal gold−silver structures before their reduction with sodium borohydride and less than 1 h for their production with PVP in ethylene glycol solution. More than 1 h of ultrasonic irradiation is required to create gold−silver worms or netlike gold−silver nanostructures capped in between with SDS either in water or propanol. After ultrasonic treatment in all cases of sonication the size of the gold particles increased. This effect was noticed for worm- or netlike gold−silver nanocomposites in the presence of SDS either in propanol or in water. XRD and ED patterns of final samples proved the presence of polycrystal gold−silver nanoalloys and their shapes discussed above.

Acknowledgment. We thank Rona Pitschke for electron microscopy analysis. This work was supported by the EU FP6 project MATSILC, the Max-Planck Society, and joined German-French laboratory "Laboratoire Européen Associé" between Max-Planck Institute and Institute of Separation Chemistry (UMR 5257 CNRS/CEA/University of Montpellier).

References and Notes

(1) Faraday, M. *Philos. Trans.* **1857**, *147*, 145−181.
(2) Turkevitch, J.; Stevenson, P. C.; Hillier. *J. Discuss. Faraday Soc.* **1951**, *11*, 55−75.
(3) (a) Frens, G. *Nature* **1973**, *241*, 20−21. (b) Hayat, M. *Electrochemistry* **1989**, *1*−*2*, 298−323. (c) Sutherland, W.; Winefordner, J. *J. Colloid Interface Sci*. **1992**, *148*, 129−140.
(4) Sezen, M.; Fisslthaler, E.; Poelt, P.; Grogger, W.; Tchernychova, E.; List, E.; Chernev, B.; Hofer, F. *Microsc. Microanal.* **2006**, *12* (2), 97−105.
(5) Creighton, J.; Blatchford, C.; Albrecht, M. *J. Chem. Soc., Faraday Trans.* **1979**, *2* (75), 790−798.
(6) Liz-Marzan, L.; Philipse, A. *J. Phys. Chem*. **1995**, *99*, 15120−15128.
(7) Kometani, N.; Tsubonishi, M.; Fujita, T.; Asami, K.; Yonezawa, Y. *Langmuir* **2001**, *17*, 578−580.
(8) Link, S.; Wang, Z.; El-Sayed, M. *J. Phys. Chem. B* **1999**, *103*, 3529−3533.
(9) Mallin, M.; Murphy, C. *J. Nano Lett.* **2002**, *2* (11), 1235−1237.
(10) Chen, Y. H.; Nickel, U. *J. Chem. Soc., Faraday Trans.* **1993**, *89*, 2479−2485.
(11) Meyers, R. A. *Encycl. Phys. Sci. Technol*. **2001**, *3*, 361−378.
(12) Vaezy, S.; Martin, P.; Goldman, B.; Chi, E.; Chandler, W.; Kaczkowski, P.; Crum, L. *Ultrason. Symp.* **1999**, *2*, 1401 − 1404.
(13) Knapp, R. T.; Daily, J. W.; Hammitt, F. G. *Cavitation* **1970**, 76−77.
(14) Le, L. Y.; Sacchi, L. H. *Ultrason. Symp.* **2004**, *1*, 565−568.
(15) Nagata, Y.; Watanabe, Y.; Fujita, S.; Dohmaru, T.; Taniguchi, S. *J. Chem. Soc., Chem. Commun.* **1992**, 1620−1622.
(16) Yeung, S. A.; Hobson, R.; Biggs, S.; Grieser, F. *J. Chem. Soc., Chem. Commun*. **1993**, 378−379.
(17) Suslick, K. S.; Fang, M.; Hyeon, T. *J. Am. Chem. Soc*. **1996**, *118*, 11960−11961.
(18) Dhas, N. A.; Suslick, K. S. *J. Am. Chem. Soc.* **2005**, *127*, 2368−2369.
(19) Didenko, Y. T.; Suslick, K. S. *J. Am. Chem. Soc*. **2005**, *127*, 12196−12197.
(20) Dibbern, E. M.; Toublan, F. J.-J.; Suslick, K. S. *J. Am. Chem. Soc.* **2006**, *128*, 6540−6541.
(21) Okitsu, K.; Ashokkumar, M.; Grieser, F. *J. Phys. Chem.* **2005**, *109*, 20673−20675.
(22) Caruso, R. A.; Ashokkumar, M.; Grieser, F. *J. Colloid Surf.* **2000**, *169*, 219−225.
(23) Salker, R. A.; Jeevanandam, P.; Aruna, S. T.; Kolyptin, Y.; Gedanken, A. *J. Mater. Chem*. **1999**, *9*, 1333−1337.
(24) Pol, V. G.; Motiei, M.; Gedanken, A.; Calderon-Moreno, J.; Mastai, Y. *J. Chem. Mater.* **2003**, *15*, 1378−1384.
(25) Suslick, K. S.; Fang, M.; Hyeon, T. *J. Am. Chem. Soc*. **1996**, *118*, 11960−11961.
(26) Li, C.; Cai, W.; Li, Y.; Hu, J.; Liu, P. *J. Phys. Chem. B* **2006**, *110* (4), 1546−1552.
(27) Pastoriza-Santos, I.; Liz-Marzan, L. M. *Nano Lett.* **2002**, *2*, 903−905.
(28) Park, J. E.; Atobe, M.; Fuchigami, T. *Ultrason. Sonochem.* **2006**, *13*, 237−241.